Open access • Journal Article • DOI:10.1364/OL.36.000178

High-performance 90° hybrid based on a silicon-on-insulator multimode interference coupler. — Source link

Robert Halir, Gunther Roelkens, Alejandro Ortega-Moñux, Juan Gonzalo Wanguemert-Perez

Institutions: University of Málaga, Ghent University

Published on: 15 Jan 2011 - Optics Letters (Opt Lett)

Topics: Multi-mode optical fiber and Silicon on insulator

High performance 90° hybrid based on a silicon-on-insulator multimode interference coupler

R. Halir,[1,*] G. Roelkens,[2], A. Ortega-Moñux[1], and J. G. Wangüemert-Pérez[1]

[1] *Departamento Ingeniería de Comunicaciones, ETSI Telecomunicación, Universidad de Málaga, 29010 Málaga, Spain*
[2] *Department of Information Technology (INTEC), Ghent University - Interuniversity Microelectronics Center (IMEC), B-9000 Gent, Belgium*
[*] *Corresponding author: robert.halir@ic.uma.es*

Compiled October 25, 2010

We propose a novel multimode interference coupler (MMI) design for high index contrast technologies, based on a shallowly etched multimode region, which is, for the first time, directly coupled to deeply etched input and output waveguides. This reduces the phase errors associated with the high index contrast, while still allowing for a very compact layout. Using this structure, we demonstrate a 2×4 MMI operating as a 90° hybrid, with a footprint of only 0.65 mm × 0.53 mm including all the structures necessary to couple light to a fibre array. The hybrid exhibits a common mode rejection ratio (CMRR) better −20 dBe and phase errors better than ±5° in a ∼ 50 nm bandwidth. © 2010 Optical Society of America

OCIS codes: (130.3120) Integrated optics devices; (230.7370) Waveguides.

MMIs are widely used devices in integrated optics, since they provide large bandwidth and relaxed fabrication tolerances. Applications include Mach-Zehnder interferometers [1], resonators [2], and 90° hybrids for coherent optical receivers [3–6]. The latter enable optical fibre based long haul transmissions with drastic increases in data rates without sacrificing additional bandwidth, by using complex quadrature and phase modulations like QPSK (quaternary phase shift keying). High index contrast technologies, such as Silicon-on-Insulator (SOI) and deeply etched Indium-Phosphide (InP) are attractive platforms for the implementation of such components, since they allow for very compact designs and small waveguide curvature radii, that allow for complex interconnections.

However, the high index contrast of deeply etched InP and SOI platforms hinders the design of high performance MMIs, as explained in the following. The basic operation of MMIs consists in launching light from one of the access waveguides (numbered 1 and 2 in Fig. 1), into the wide multimode section where it expands into multiple modes. These travel with different propagation constants, and, at certain imaging distances, interfere to form one or several replicas of the input field, which are coupled to the output waveguides (numbered 3 to 6 in Fig. 1). The formation of these images is governed by the self-imaging theory [7], which essentially requires that all the modes excited in the multimode section exhibit quadratically related propagation constants, i.e. $\beta_m = \beta_1 - (m^2 - 1)\pi/(3L_\pi)$, where $m = 1, 2, 3, ...$ is the mode number and L_π is the beat length of the two lowest order modes. In waveguides with high lateral (x direction) index contrast, such as deeply etched InP ridges and silicon wires, this relation between the propagation constants only holds for the lower order modes, resulting in strong phase errors for the higher order modes [8]. These phase errors result in low quality imaging, and become especially detrimental as the number of MMI inputs or outputs grows.

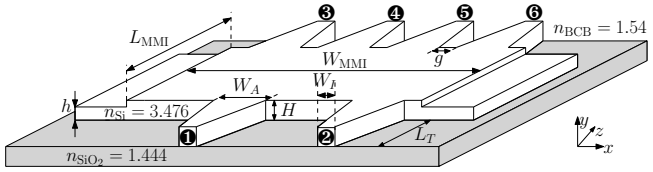

Fig. 1: Schematic drawing of the proposed MMI geometry. Refractive indexes are given at $\lambda = 1.55\,\mu$m.

A number of techniques have been proposed to overcome this problem. First, by increasing the access waveguide width, only the lowest order modes, which exhibit almost ideal propagation constants, are excited [9–12]. This requires careful design of the access waveguide width, since increasing it too much results in unnecessarily large devices [9]. Second, using shallowly etched waveguides [8] reduces the index contrast, thus alleviating the phase error. However, this yields larger devices, since the shallowly etched input and output waveguides need to be further separated to avoid coupling between them, and sacrifices the small curvature radii. Finally, simulations of MMIs with engineered, quasi-optimum refractive index profile in the multimode region show compact, high performance devices [13]. Yet, the engineered refractive index profile is difficult to implement.

Here we propose a novel MMI design, operating as a 90° hybrid, that achieves good imaging quality while maintaining compactness typical for high index contrast technology. Using silicon wire technology we demonstrate, for the first time, the use of a shallowly etched multimode region coupled directly to deeply etched waveguides, that exhibit tight curvature radii and allow a dense spacing. Experimental results confirm the excellent performance of the device.

The proposed design is shown in Fig. 1. The silicon core layer is $H = 220\,\text{nm}$ thick, and the single mode interconnecting waveguides are $W_I = 450\,\text{nm}$ wide. The minimum gap between the output waveguides is set to $g = 500\,\text{nm}$ to avoid coupling between them, and DVS-BCB (divinyl siloxane bis-benzocyclobutene) is used as cladding material. The access waveguides are completely etched, but the multimode region is only etched to a depth of $D = H - h$, to reduce the index contrast.

To determine the optimum etch depth of the multimode region, we calculated the propagation constants of its TE polarized modes for a fixed width $W_{\text{MMI}} = 7.7\,\mu\text{m}$, using a commercial modesolver. The accumulated phase error at the 4-fold imaging distance, $(3/8)L_\pi$, was then computed for each mode. Fig. 2 shows the phase error as a function of mode propagation angle for different heights (h) of the lateral slab. From Fig. 2 it is clear that a fully etched ($h = 0\,\text{nm}$) multimode region yields very large, negative, phase errors. Reducing the etch depth, i.e. increasing h, reduces the maximum possible propagation angle in the multimode region, but it also drastically reduces the phase error of the modes that remain guided. Reducing etch depth below 70 nm ($h > 150\,\text{nm}$), again produces increased, positive, phase errors. Thus, the etch depth was fixed at 70 nm ($h = 150\,\text{nm}$), which also makes the fabrication of the devices compatible with the definition of the fibre-to-chip grating couplers, which are etched 70 nm deep into the silicon waveguide layer [14].

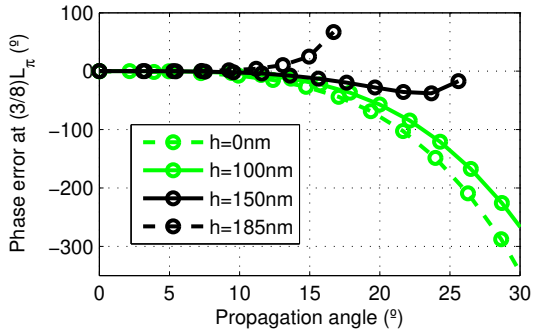

Fig. 2: Deviation from the ideal phase as a function of modal propagation angle for different heights of the lateral slab (h).

Despite using a shallowly etched multimode region, here we propose the use of fully etched access waveguides. While this may seem counterintuitive, it has several advantages. First, it reduces coupling between the output waveguides, so that they can be placed closer toghether, reducing the footprint of the device. Second, it obviates the need of a transition between the fully etched interconnecting waveguides and the shallowly etched multimode region. Finally it enables the use of tight bends in the input and output waveguides. In [9] it was shown that low-loss coupling of the access waveguides requires that the input mode profile exhibit the same symmetry in the vertical direction as the modes supported by the multimode region. Fig. 3 shows that, as expected, the mode field of the input waveguide is virtually symmetric in the vertical direction. The mode fields of the multimode region, despite being shallowly etched, exhibit the same type of symmetry, with the exception of the edge of the device, where the field is distorted, due to the presence of the lateral slab. Since the input and output waveguides are not placed at the edge of the multimode region, low-loss coupling is feasible. However, due to the reduced index contrast, the multimode region only supports a limited number of modes. Consequently the input waveguide width has to be designed such that only the guided modes are excited. Eigenmode expansion simulations show that a waveguide width of $W_A = 1.5\,\mu\text{m}$ ensure that at least 98 % of the incident power couples into guided modes of the multimode region. The width (W_{MMI}) and length (L_{MMI}) of the multimode region were iteratively optimized to yield minimum imbalance and insertion losses. The resulting dimensions are $W_{\text{MMI}} = 7.7\,\mu\text{m}$ and $L_{\text{MMI}} = 115.5\,\mu\text{m}$.

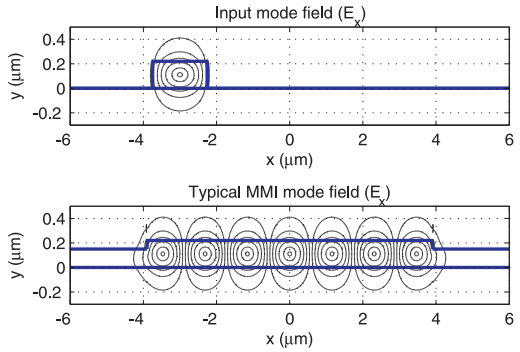

Fig. 3: Mode field of the fully etched access waveguide (upper figure) and of one of the modes of the shallowly etched multimode region (lower figure).

For testing purposes TE polarized light is coupled in and out of the chip with grating couplers. To facilitate accurate characterization, the 2×4 MMI was embedded into the following test structure. The light coupled into the chip is divided by a 1×2 MMI. One of the 1×2 MMI outputs is fed directly into input 1 of the 2×4 MMI, whereas light from the other output travels through a delay line before entering input 2 of the 2×4 MMI. When scanning the input wavelength, this delay creates an interferogram at each of the 2×4 MMI outputs from which its amplitude and phase characteristics can be obtained [15, 16]. The input and output gratings were aligned so that they are accessible with a fibre array, enabling simultaneous detection of the four outputs. The complete test structure occupies an area of $0.65\,\text{mm} \times 0.53\,\text{mm}$, which is essentially determined by the $127\,\mu\text{m}$ spacing of the fibres in the array.

The device was fabricated on a silicon-on-insulator wafer with a silicon thickness of 220 nm using deep UV lithography and a two etch depth process. A 70-nm etch

was used for the multimode region and the grating couplers, whereas the photonic wires were fully etched.

A 90° hybrid ideally combines the waves from its two inputs with the same amplitude at each output, and with relative phases that differ by 90° from output to output. This behaviour is usually quantified with two parameters, the common mode rejection ratio and the phase error. Denoting by p_i the power at each output, the CMRR for the in-phase channel is defined as $\mathrm{CMRR\,[dBe]} = 20\log_{10}\frac{p_3-p_6}{p_3+p_6}$, when power is launched from either input [the CMRR is measured in electrical decibels (dBe), hence the factor 20]. For the quadrature channel p_3 and p_6 are substituted by p_4 and p_5, respectively. The phase error is the deviation from the ideal 90° shifts between the outputs. Fig. 4(a) shows the measured CMRR of the device in the 1500 nm – 1560 nm band, which is well below −20 dBe in a 45 nm bandwidth. The phase error is within ±5° in a 55 nm bandwidth [see Fig. 4(b)]. The device thus readily matches the performance of state of the art 90° hybrids, which have footprint up to 20 times larger [5,6]. The inset in Fig. 4(a) shows the relative amplitudes and phases with which the hybrid combines the waves from the two inputs at each output.

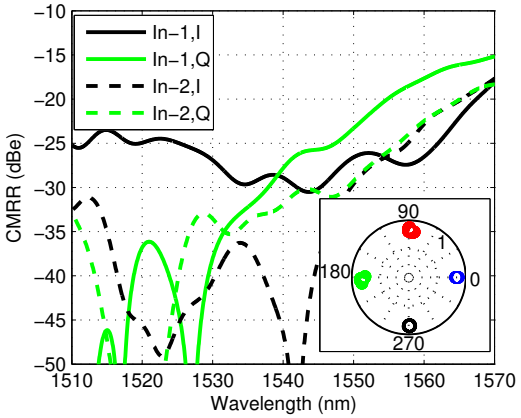

(a)

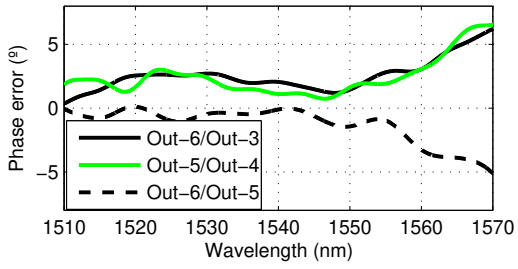

(b)

Fig. 4: (a) CMRR of the fabricated device as a function of wavelength. The inset shows the relative amplitude and phase with which the waves from the two inputs combine at each output. (b) Phase error between outputs as a function of wavelength.

We have proposed and demonstrated a novel MMI design for high index contrast platforms, based on a shallowly etched multimode region to reduce the modal phase error, and deeply etched access waveguides to allow for a compact overall layout. A 90° hybrid based on this design exhibits excellent performance, and an ultra-compact footprint. While the concept is demonstrated here in silicon technology, it is directly applicable to other platforms, such as deeply etched InP.

This work has been supported by the Spanish Ministerio de Ciencia e Innovación under project TEC2009-10152, a FPU scholarship AP-2006-03355, and by the Andalusian Regional Ministry of Science, Innovation and Business under project TIC-02946.

References

1. D. Kim, A. Barkai, R. Jones, N. Elek, H. Nguyen, and A. Liu, Opt. Lett. **33**, 530 (2008).
2. D.-X. Xu, A. Densmore, P. Waldron, J. Lapointe, E. Post, A. Delâge, S. Janz, P. Cheben, J. Schmid, and B. Lamontagne, Opt. Express **15**, 3149 (2007).
3. L. Zimmermann, K. Voigt, G. Winzer, K. Petermann, and C. Weinert, IEEE Photonics Technol. Lett. **21**, 143 (2009).
4. R. Kunkel, H.-G. Bach, D. Hoffmann, C. Weinert, I. Molina-Fernandez, and R. Halir, in *Indium Phosphide & Related Materials, 2009. IPRM '09.* (IEEE Photonics Society, Newport Beach, CA, USA, 2009), pp. 167–170.
5. S. Jeong and K. Morito, Opt. Express **18**, 4275 (2010).
6. H.-G. Bach, A. Matiss, C. Leonhardt, R. Kunkel, D. Schmidt, M. Schell, and A. Umbach, in *Optical Fiber Communication Conference* (2009), pp. 1 –3.
7. M. Bachmann, P. Besse, and H. Melchior, Appl. Optics **33**, 3905 (1994).
8. J. Huang, R. Scarmozzino, and R. Osgood, IEEE Photonics Technol. Lett. **10**, 1292 (1998).
9. R. Halir, I. Molina-Fernández, A. Ortega-Moñux, J. G. Wangüemert-Pérez, D.-X. Xu, P. Cheben, and S. Janz, J. Lightwave Technol. **26**, 2928 (2008).
10. R. Halir, A. Ortega-Moñux, I. Molina-Fernández, J. G. Wangüemert-Pérez, P. Cheben, D.-X. Xu, B. Lamontagne, and S. Janz, IEEE Photonics Technol. Lett. **21**, 1600 (2009).
11. D. J. Thomson, Y. Hu, G. T. Reed, and J.-M. Fedeli, IEEE Photonics Technol. Lett. **22**, 1485 (2010).
12. A. Hosseini, H. Subbaraman, D. Kwong, Y. Zhang, and R. T. Chen, Opt. Lett. **35**, 2864 (2010).
13. I. Molina-Fernández, A. Ortega-Moñux, and J. G. Wangüemert-Pérez, J. Lightwave Technol. **27**, 1307 (2009).
14. G. Roelkens, D. Vermeulen, F. V. Laere, S. Selvaraja, S. Scheerlinck, D. Taillaert, W. Bogaerts, P. Dumon, D. V. Thourhout, and R. Baets, J Nanosci Nanotechno **10**, 1551 (2010).
15. R. Halir, I. Molina-Fernández, J.G.Wangüemert-Pérez, A. Ortega-Moñux, J. de Oliva-Rubio, and P. Cheben, Opt. Express **17**, 8349 (2009).
16. R. Halir, A. Ortega-Moñux, I. Molina-Fernández, J. G. Wangüemert-Pérez, P. Cheben, D.-X. Xu, B. Lamontagne, and S. Janz, J. Lightwave Technol. **27**, 5405 (2009).